Fish behaviour and orientation dependent backscatter in acoustic Doppler profiler data

L. Zedel, R.K. Patro, T. Knutsen

Abstract - It is well known that fish target strength can be affected by fish behaviour. In particular, the specific orientation between a target (fish) and an echosounder system is critical in interpreting the apparent target strength. This situation is further complicated for Doppler current profiler systems which have an array of diverging beams and where each beam will interact with targets with a different orientation. When targets themselves have random orientations, each beam will see the same range of target strengths and the average values would be the same. However, if targets such as schooling fish have a preferred orientation, then an asymmetry is present and different target strengths can be expected. This hypothesis is explored using observations of Norwegian Spring Spawning Herring (Clupea harengus) under a variety of schooling conditions. When schooling fish are migrating horizontally and have well defined coherent orientations, differences in backscatter strength of about 5 dB can be seen depending on beam orientation. This difference disappears when fish are not actively migrating and so do not have coherent orientation. These differences can be used to infer behaviour of schooling fish but they also indicate that caution must be exercised when averaging backscatter data from separate ADCP beams.

Keywords: ADCP, Norwegian herring, target strength, fish behaviour

Len Zedel: Department of Physics and Physical Oceanography, Memorial University of Newfoundland, St. John's, Nf, A1B 3X7, Canada [e-mail: zedel@physics.mun.ca. Ranjan Patro: Department of Physics, College of the North Atlantic, Labrador City, NL, A2V 2Y1, Canada [e-mail]: Ranjan.Patro@northatlantic.nf.ca. Tor Knutsen: Institute of Marine Research, PO Box 1870 Nordnes, 5817 Bergen, Norway [e-mail: tor@imr.no].

1 Introduction

Acoustic Doppler current profiler (ADCP) systems have become a standard tool for oceanographers and data from these instruments has now become generally available. In addition to generating current profiles these instruments can be configured to record acoustic backscatter profiles that are normally used to evaluate quality of the velocity profiles. However, the existence of the backscatter data provides the attractive opportunity for use in biological surveys; see for example Flagg and Smith (1989), Ashjian et al. (1994). It is also possible to combine the velocity and backscatter data to infer fish behaviour (Demer et al. (2000), Zedel et al. (2003) and Lee (2004)). However, proper deployment of these instruments for biological applications requires accurate calibration of acoustic backscatter and this has proved difficult with existing systems (see Brierely et al. (1998), Fielding et al. (2004), and Ressler (2002)).

The deployment geometry of the ADCP with (typically) four diverging beams requires some special consideration and can be expected to affect the data interpretation (as noted by Griffiths et al. (2002)). However, the availability of separate beams sampling the same (or similar) water volume should provide additional information on scatterer characteristics. Analysis of differences between backscatter levels in ADCP beams forms the focus of the present paper.

Typical ship mounted fisheries sonar systems have beams that interrogate targets from a vertical orientation. Target strength can depend on fish behaviour but because of the vertical symmetry of the beam it does not depend on the direction of motion of the fish with respect to the sonar system. This situation is indicated in Figure 1 by the vertical dashed line and the sketched directivity function of the fish backscatter: for a given tilt angle, the detected target strength will not depend on the swimming direction of the fish. The situation is different for acoustic beams directed off of vertical, consider the interaction between the solid arrows and the directivity function in Figure 1; depending on whether the fish is swimming toward or away from the beam a difference in target strength will be realised. In considering Figure 1 also notice that if the directivity function were symmetrical with respect to the vertical (ie. not tilted away from a vertical orientation) there again is no dependence on swimming direction even with the tilted acoustic beams.

Individual beams will never sample the same target at the same time so that the consequences of differences in target strength will only appear in averaged data. If the targets themselves assume random orientations, then the averages seen by the separate beams will not be different. A separate question that may be asked is what the averages mean given the dependence on target orientation. For schooling fish where swimming directions of many individuals are aligned it should be possible to distinguish systematic differences between averaged target strengths from separate acoustic beams.

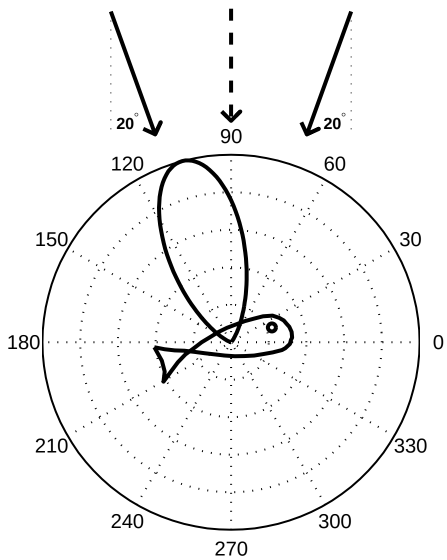

Figure 1: Geometry of target with asymmetrical directivity function sampled by vertical sonar (dashed arrow) and oblique sonar beams (solid arrows).

In order to explore the dependence on beam orientation that might arise in ADCP data, observations of schooling fish of well defined behaviour are required. Observations of migrating and overwintering Norwegian Spring Spawning Herring (*Clupea harengus)* in the Lofoten area of Norway (see Figure 2) provide just such an opportunity. Here, herring are known to have a directivity function that is not symmetrical with respect to swimming direction (Foote and Nakken (1978)). Target strength for these fish are further complicated by diurnal and depth dependent behaviour (Huse and Ona (1996)). During the day they stay in deep water to avoid visual predators: at depth, they have reduced buoyancy and so they must assume a “tilt” to their swimming attitude in order to maintain depth (Huse and Ona (1996)). During the night they approach the surface where they may refill their swim bladders and also find a depth of neutral buoyancy thereby reducing energy requirements (Blaxter and Batty (1984)).

2 Method

2.1 Deployment Configuration

Details of the ADCP observations in the Ofoten region of Norway can be found in Zedel et al. (2003). An RD Instruments 307 kHz WorkHorse ADCP was positioned at mid-depth on a mooring configured to have the $\simeq$ 150 m sampling range of the instrument detect large schools of herring. The instrument has four acoustic beams (of 2.2° beam width) directed downward 20° from vertical. The deployment configuration is shown schematically in Figure 3. The ADCP was configured with a 2.36 m long transmit

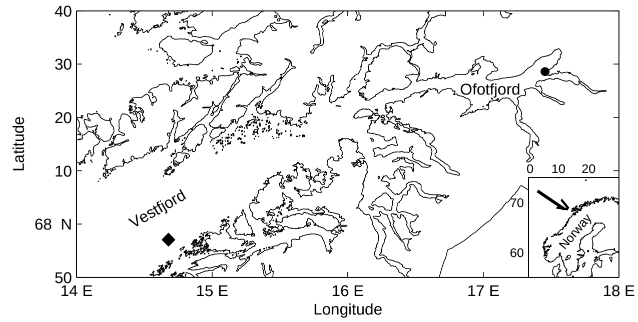

Figure 2: Map of deployment area on the Norwegian coast, ● indicates the location of Deployment Dep9704 (03:00 to 12:30 CET 7 December, 1997) and ◆ indicates the location of deployment Dep9804 (11:47 to 17:07 CET, 28 January 1998).

pulse and data was collected in 75 2-m depth bins: data was recorded in beam coordinates so that data from individual beams could be analysed. RD Instruments provides an algorithm that rejects fish contaminated data by comparing backscatter levels between the various beams: this algorithm does not affect data when collected for individual beams. the instrument transmit interval was set to 10 seconds in the 1997 data and 5 seconds in the 1998 data with no averaging of profiles. Observations during December 1997 are of overwintering herring so that the fish schools are not moving quickly (Zedel et al. (2003)). In contrast, observations made in January 1998 are of herring that have begun their southward migration. At this time the schools are moving with a well defined direction with an average speed of 20-30 cm s^{-1} (Zedel et al. (2003)) and the fish can be expected to maintain a well defined swimming direction.

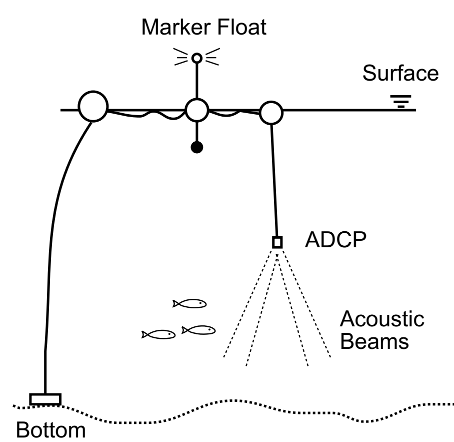

Figure 3: Geometry of ADCP deployment.

2.2 Calibration

Before any comparison of backscatter between the beams can be made, it is necessary to calibrate backscatter from the four beams. Deines (1999) provides a detailed description of calibration procedures and system constants suitable for the RD Instruments ADCP systems. Backscatter strength in dB re 1 m^{-1} for these systems can be determined as:

$$S_v = c + 10\ log_{10}(T_x + 273.16)R^2 - L_{DBM} - P_{DBW} + 2\alpha R + K_c(E - E_r) \quad (1)$$

where c is a sonar configuration scaling factor, (for the Workhorse sentinel $c = -143.5$ dB); this term includes the system source level, transducer directivity, transducer efficiency and the Boltzmann constant (used in scaling the thermal noise to an absolute level), T_x is the temperature at the transducer in °C, R is the (slant) range to the sample bin in m, $L_{DBM} = 10\,log_{10}(L)$, L is the transmit pulse length in meters, $P_{DBW} = 14 = 10\,log_{10}(P)$, P is the transmit power in dB re 1 Watt, α is the sound absorption coefficient = 0.0873 dB/m (at 4° C, 307 kHz), $K_c \simeq 0.45$ dB/LSB is the instrument sensitivity, E is the recorded backscatter signal, and E_r is the minimum (background) level recorded by the instrument.

The instrument sensitivity (K_c) varies from beam to beam and between instruments and should normally be measured to achieve the best accuracy. Such measurements could not be acquired for the present instrument and we are forced to use the default value of 0.45 dB/LSB.

2.3 Calibration Check

In order to validate the consistency of the beam calibrations, data from a test survey were used to compare backscatter from the four beams. Data were collected in a protected fjord near the University of Bergen, Espegrende field station. The ADCP was deployed from a launch and lowered to a depth of 50 m (simulating the actual field deployment). The instrument was then towed at a speed of 0.5 $m\,s^{-1}$ in directions 15°, 115°, 195°, and 270° (true) holding the course steady for 5 minutes in each direction thereby describing a square pattern. Data collected while the tow direction was being changed were discarded. Through this trial, the wire angle to the suspended ADCP was about 10° from vertical; the instrument roll was less than 5° and pitch was less than 1°. By following this sampling procedure, each of the four beams will interact with the scatterers with the same four angles (in the horizontal). Assuming that conditions in the fjord did not change over the 30 minute period of the test, the average of backscatter level in each of the four beams should be the same. Example profiles from the four beams are shown in Figure 4: the maximum range displayed is for 130 m as data beyond this range was contaminated by a bottom reflection. The averages presented in Fig. 4 are of logarithmic values (a geometric average); averages of linear values provide similar results but show increased noise because of the presence of outliers in the data probably caused by fish. By using a logarithmic average, these few large amplitude anomalies do not dominate the final average value as they would in a linear average. Figure 4 demonastrates that by using the default value of 0.45 dB/LSB for the instrument sensitivity (K_c), differences in backscatter between the four beams are less than ± 0.5 dB. This result is as accurate as can be expected given the 0.45 db/LSB resolution of the instruments and for this reason, no adjustments of the default instrument calibration has been applied.

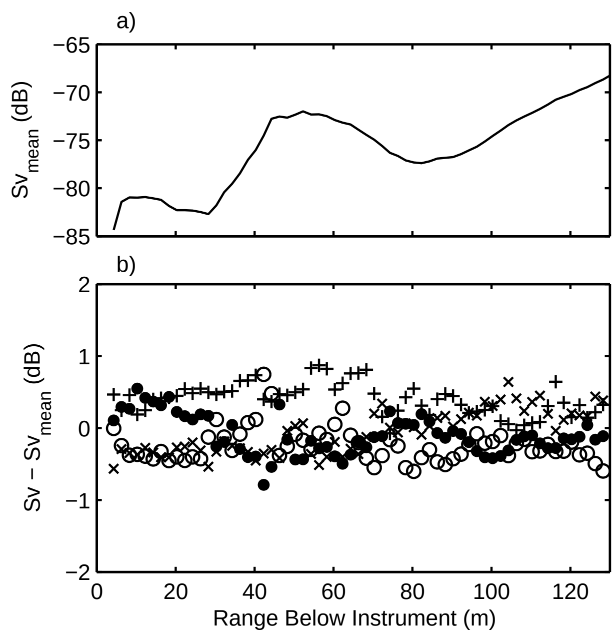

Figure 4: Results of calibration test; a) average backscatter with depth, b) difference between average backscatter and individual beam data: • beam 1, ○ beam 2, × beam3, and + beam 4.

2.4 Beam Orientation

In the freely drifting deployment used for the present observations, it is impossible to control the exact attitude of the ADCP. In fact, few ADCP deployment configurations allow for control of the instrument attitude and for this reason the instruments record attitude by measuring heading, pitch and roll. The changes in instrument attitude affect the beam interaction angles slightly (relevant to the present discussion), but more importantly, they change the relationship between range along the acoustic beams and depth below the instrument. In order to accurately compare backscatter from a given depth (which we assume is horizontally uniform), we must correctly account for beam orientation. The transformation matrix used to correct for beam orientation is described in Appendix A.

An example of the effect of applying rotation corrections to the beams is shown in Figure 5: 5a shows the average (corrected) backscatter observed during a one hour period on 27 January 1998. Figure 5b shows the -55 dB contours in backscatter (S_v) from opposite facing beams 1 and 2 before corrections showing an obvious mismatch of as much as 10 m in the location of strong backscatter. Through this deployment, the ADCP recorded an average pitch of 2.5° and a roll of -6°. In Figure 5c, the rotation corrections have been applied and the -55 dB contours are noticeably better aligned although small differences are still apparent.

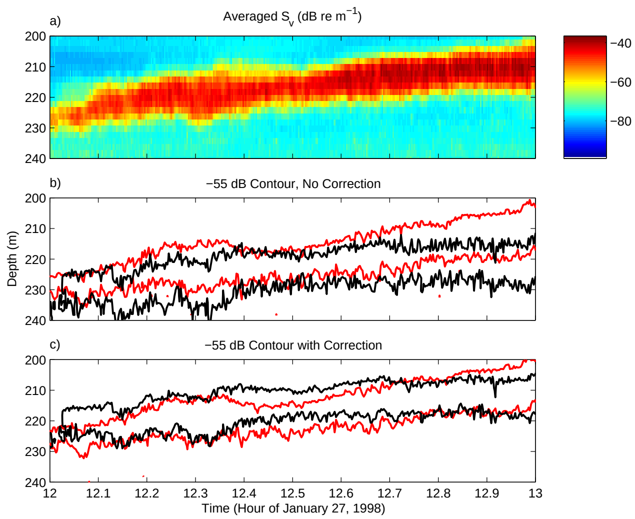

Figure 5: a) Averaged values of S_v observed during a one hour period on 27 January 1998. b) Contours of the -55 dB S_v levels from the opposite facing beams 1 (red) and 2 (black) before correction for rotation. c) Contours of the -55 dB S_v levels from the opposite facing beams 1 (red) and 2 (black) after correction for rotation.

2.5 Fish Orientation

The orientation relationship between the ADCP beams, and the fish swimming direction is shown by an example in Figure 6 where the ADCP heading is 20°(True) and the fish swimming direction is identified as 90°(True). The orientation direction (in the horizonatal plane) for each of the ADCP beams is indicated by arrows labeled B1, B2, B3, and B4 for beams 1 to 4; they have headings of 290°, 110°, 20°, and 200° respectively (with respect to true north). For the purposes of the present discussion, the angle between the individual ADCP beams and the fish swimming direction is important and we use the difference value, beam heading minus fish heading (beam-fish interaction angle). For the example of Figure 6, beam-fish interaction angles are 290° - 90° = 200°, 100° - 90°= 20°, 20° - 90°= -70°, and 200° - 90° = 110° for beams 1 through 4. All beam-fish interaction angles are reported as between 0° and 360°: when negative angles occur those values are reported as an equivalent positive value. In the present example, the -70° interaction angle given for beam 4 would be replaced with -70° + 360° = 290°.

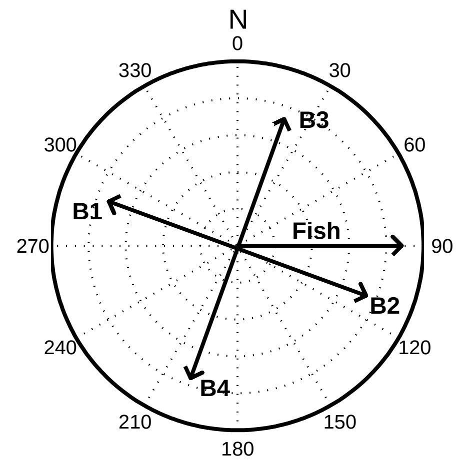

Figure 6: Example relationship between ADCP instrument heading (of 20° True) and sampling directions of acoustic beams 1 through 4 labelled B1, B2, B3, and B4.

3 Sorting Data

In order to evaluate backscatter dependence on beam orientation, backscatter data have to be organised by the interaction angle between the sonar system and the fish. It is not possible to extract the swimming direction of a single fish with an ADCP system because the instrument relies on data from beams sampling separate regions of water. The approach that we use is to determine the direction of movement of a fish school as a whole and to use that direction to provide a time series of fish swimming direction. The process of extracting this information is presented through the following analysis of migrating fish data.

3.1 Migrating Fish

The herring school is identified in ADCP data from the -55 dB contour in the average of backscatter from the four beams. The -55 dB cutoff is used because it clearly delineates the school of herring and it is consistent with backscatter levels expected from herring. Time series of fish swimming speed and direction are then determined by averaging these values over all depths for which schooling herring are identified (by the -55 dB threshold). Doppler velocities are amplitude weighted within a ping so that in regions of backscatter caused by herring, the velocity that is determined will be that of the herring and not that of the water. Figure 7a shows the herring school observed on January 27, 1998 from 12:00 to 15:30: identifying the fish school from the -55 dB threshold in S_v Figures 7b and c provide the speed and direction observations within the fish school. The velocity data identified for herring in Figures 7b and c were averaged over depth to produce velocity data for the school (shown in Figures 8c and d). There are few speed and direction values identified between 13:15 and 14:30 because average backscatter level does not exceed the -55 dB criterion through this interval.

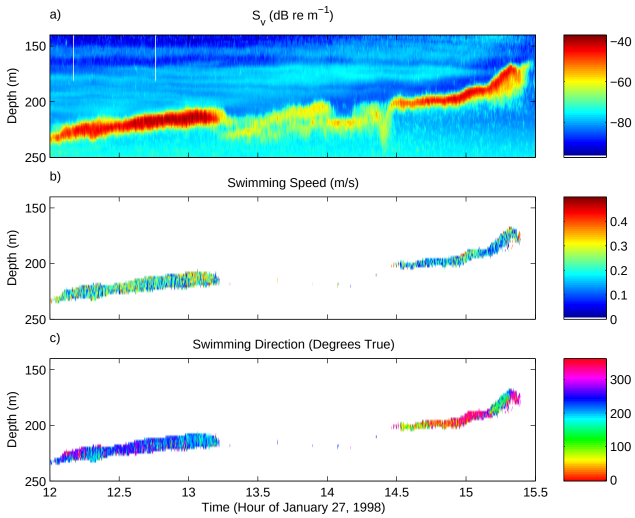

Figure 7: a) Beam averaged, depth corrected backscatter for deployment January 27, 1998. b) Swimming speed of detected fish ($S_v > -55$). c) Swimming direction of detected fish.

The fish school as detected by the -55 dB contour in individual beams is now used to provide time series of backscatter for each beam. Data from beams 1 and 2 shown in Figure 8 demonstrate the differences in backscatter that occurs between the beams. These beams have been selected because they face in opposite directions: only two beams are shown to minimise clutter in the figure. Notice that the relative differences are not consistent through the record: at first, beam 1 levels are higher but toward the end of the record, beam 2 levels are the highest. What changes during the deployment is the orientation of the beams with respect to the swimming direction of the fish. Figure 8b shows the instrument heading through the deployment and Figures 8c and d show the swimming direction of the fish and their average speed. There is no speed and direction data through the interval from hour 13.25 to hour 14.5 in Figure 8 because of inadequate data returns through this time period; data from this time interval is not used in subsequent analysis.

The time series presentation of Figure 8 demonstrates that differences in backscatter do occur between the beams, but the changes that occur with time make it difficult to identify any systematic dif-

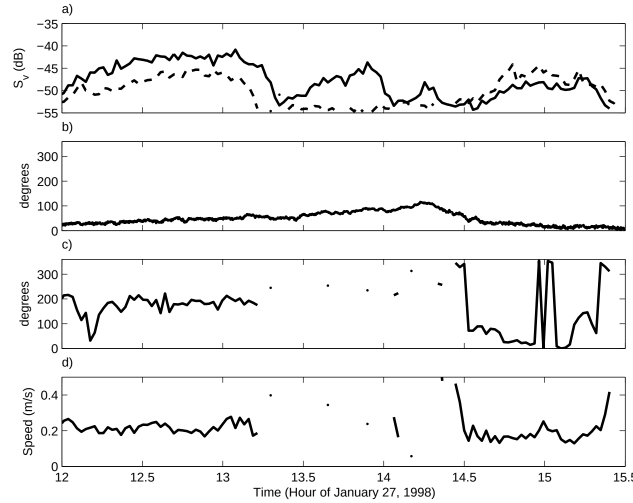

Figure 8: a) Backscatter from beam 1 (solid) and beam 2 (dashed) over 4 hour period on January 27, 1998. b) Instrument heading. c) Fish swimming direction. d) Fish swimming speed.

ferences. In order to remove the time varying component, an average was determined from the four beams;

$$S_{v-av} = (S_{v1} + S_{v2} + S_{v3} + S_{v4})/4 \quad (2)$$

where S_{vn} is the backscatter recorded for beam n (n = 1 to 4). The difference between the average and the individual beam data was then considered;

$$\delta S_{vn} = S_{vn} - S_{v-av}, \quad (3)$$

where again, n takes values of 1 to 4. The values of δS_{vn} were averaged according to the difference between beam heading and fish swimming direction for each beam using 10° intervals and the results are shown in Figure 9. What Figure 9 indicates for each beam at any given direction is whether backscatter levels were higher or lower than the average over the four beams.

Figure 9 shows that a clear difference in (relative) backscatter strength occurs as a function of beam-fish interaction angle. Fish traveling away from the beam have backscatter that is about 5 dB greater than those that are traveling toward a beam. No one beam provides information through the entire 360° of interaction angles but there is substantial overlap and through these regions there is agreement between the duplicating beams. Data from a second similar deployment on January 29 gives a similar result with a 6 dB response difference. (During this deployment, instrument pitch was about 2° and roll was -4°.)

3.2 Overwintering Fish

The data presented in Figure 9 are representative of migrating fish schools when fish would be expected

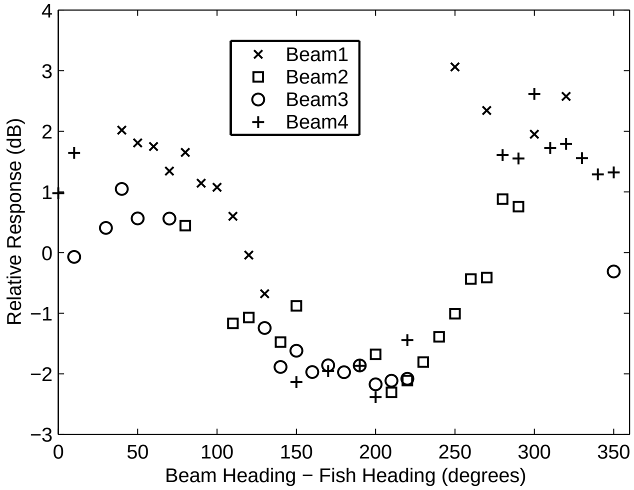

Figure 9: Beam response (relative to the mean of the four ADCP beams) with respect to beam-fish interaction angle.

to have well defined, coherent orientation. Backscatter dependence on orientation should not be expected when fish do not have coherent motion. In order to further test the presented hypothesis, backscatter data from overwintering herring collected in Ofotfjord during 7 December 1997 were analysed using the same approach as that described for the migrating fish.

A summary of the fish observations is shown in Figure 10 similar to that of Figure 7; Figure 10a shows the (beam averaged) backscatter after calibration and correction for rotations, Figure 10b and c show the swimming speed and direction of the fish as detected by the -55 dB contour in S_v. For this deployment, the ADCP recorded an average pitch of -1.5° and a roll of -2°. In this 6 hour record, the fish school starts out somewhat dispersed and then coalesces (at around 10:30) into a more well defined group that ranges in depths from 60 m to 140 m. For most of this deployment, the fish swimming speeds are low with little apparent difference between fish speed and that of the water (see Zedel et al. (2003)). The direction of motion (Figure 10c) shows that the swimming direction wanders around significantly through the observations particularly at the end of the deployment.

These data were again sorted according to relative backscatter as a function of fish-beam interaction angle (Figure 11). The form of the data again show an increase in S_v for fish swimming away from the beams but in this case, the increase is only about 0.5 dB and not significant given the 0.45 dB/LSB resolution of the recievers. All four beams show interactions through 360 degrees for this deployment and all agree in the form and approximate magnitude of the difference. Selecting subsets of this deployment does

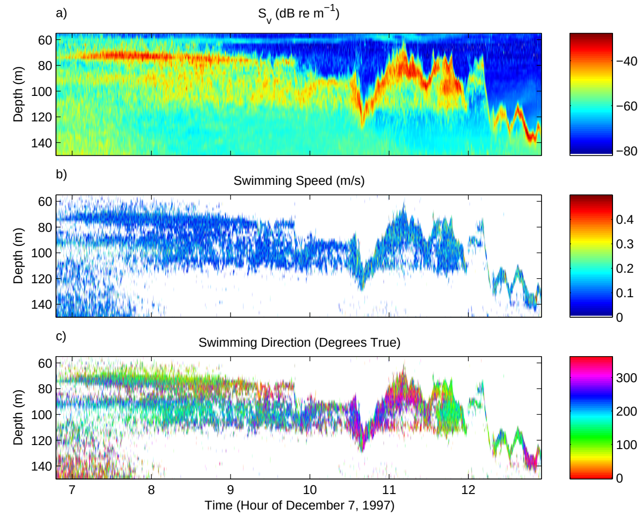

Figure 10: a) Beam averaged, depth corrected backscatter for deployment 7 December 1997. b) Swimming speed of detected fish ($S_v > -55$ dB). c) Swimming direction of detected fish.

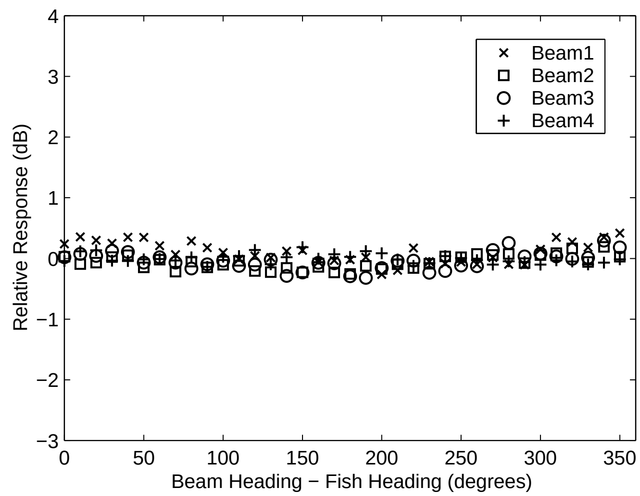

Figure 11: Beam response (relative to the mean of the four ADCP beams) with respect to beam-fish interaction angle.

not increase the backscatter variability.

4 Discussion

The hypothesis underlying the present analysis is that the directional target strength of fish could (in certain circumstances) lead to differences between the backscatter observations of the diverging ADCP beams. The data presented in Figures 9, and 11 support this hypothesis and imply that the target strength directivity function of herring is asymmetrical with respect to vertical (see Figure 1).

Measurements of herring scattering directivity are reported by Foote and Nakken (1978) for 30 herring ranging in length from 8.7 cm to 32.4 cm at 120 kHz. The average directivity function for these data is indicated by the solid line in Figure 12 where positive tilt angle corresponds to a fish swimming forward and upward as indicated in Figure 1. The interesting thing that is immediately apparent in the backscatter data of Foote and Nakken (1978) for herring is that it is asymmetrical with respect to the vertical.

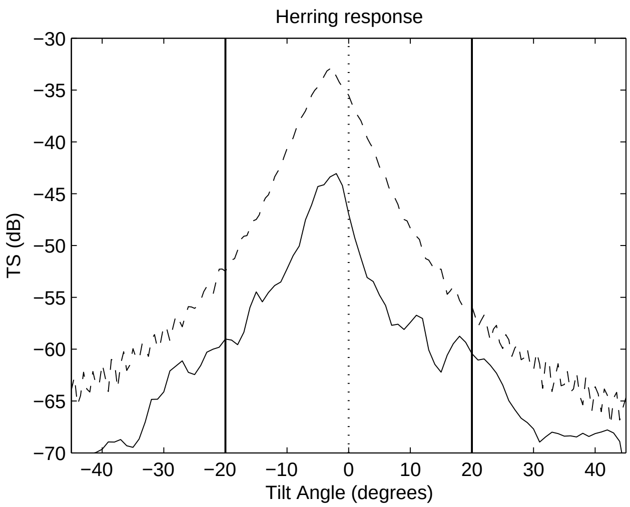

Figure 12: Backscatter directivity response of herring based on experiments by Foote and Nakken (1978)for a 120 kHz sonar (solid line), and model predictions for a 307 kHz sonar from a 33 cm herring (dashed line) using the approach described by Chu et al. (2003). The model data have been offset by 3.5° to match the experimental observations. Solid vertical lines at $\pm 20^\circ$ indicate the interaction angle expected for ADCP beams.

Directivity is of course sensitive to frequency and the present data were collected using a 307 kHz system so that direct comparison with the data of Foote and Nakken (1978) is not possible. In this case we use the results of the scattering model described by Chu et al. (2003) for a 33 cm herring with a 8.3×0.87 cm swim bladder (consistent with the values used by Gorska and Ona (2003)) at 307 kHz and this is indicated by the dashed line in Figure 12. The model data has been offset in tilt by 3.5° to match the offset seen in the 120 kHz observations. As is expected, the form of the model prediction is very similar to that of the direct observations differing primarily in overall level. In the present ADCP observations, ignoring the pitch and roll, the acoustic beams would sample a horizontally swimming fish at an equivalent tilt angles of 20° for a fish moving toward the ADCP and -20° for fish moving away from the ADCP (these values are drawn in Figure 12 by vertical lines). The difference between the $\pm 20^\circ$ target strengths is about 5 dB with higher levels indicated for fish swimming away from the instrument and this is consistent both in sign and magnitude to the present observations.

In considering the directional backscatter characteristics from herring the tilt distributions for the fish have been ignored. This assumption is not always valid because the swimming behaviour of herring can be quite variable with (mean) tilt angles as high as 40° and at times giving rise to bimodal tilt distributions (Huse and Ona (1996)). Huse and Ona (1996) did observe that when there is sufficient light for schools to form and at depths below 200 m, herring were swimming horizontally. It is most likely that the migrating fish in the present observations are swimming horizontally. In the case of the overwintering fish, data span the transition through dawn. The formation of a well defined school in Figure 10 at 10:30 is probably triggered when light levels become adequate for schooling to occur. In the school, the fish are probably oriented horizontally (Huse and Ona (1996)) but earlier on in the record this may not be the case. Recognising that the data from this deployment may include times of different fish behaviour, the analysis was repeated looking for response differences from the interval 6:48 to 10:30 and then from 10:30 to 12:55. Neither of these subsampled data sets show any increased response to beam directions and because less data is included in the averages, the results show greater scatter. It is of course possible that different processes cause the degradation of beam orientation effects at different times during this deployment: tilt angle distributions may be a factor during the early part of the record.

A concern with the sorting of the data was that depending on the deployment, the ADCP would have a significant pitch or roll. For example, during the deployment shown in Figure 7 for migrating fish, the pitch was about 2° and roll was -4°. In this instance, the angle of the acoustic beams 1 to 4 with respect to vertical would be 16°, 24°, 18° and 22° respectively. These tilts are significant compared to the 3.5° offset from vertical of the herring directivity function seen by Foote and Nakken (1978). We have not accounted for these additional angular variations because there is insufficient data to fully explore this second angular degree of freedom: in effect we would be attempting to reconstruct a complete two dimensional directivity function. The fact that the pitch and roll do not dominate the analysis can be seen by considering Figure 9 and noting that significant duplication of the diagram occurs with each individual beam.

5 Conclusions

In this paper we have shown that significant systematic differences in backscatter can occur between the beams of an ADCP. In the present case, these differences depend on the angle between the beam orientation and the swimming direction of Norwegian spring spawning herring (*Clupea harengus*). The observed difference of 5 dB greater backscatter when fish were swimming away from the beam as compared to fish swimming toward the beam is consistent in sign and magnitude with backscatter directivity of Norwegian herring. Analysis of calibrated ADCP backscatter clearly depends on fish behaviour and can therefore provide information on the behaviour of schooling fish.

In order to observe these orientation dependent effects, it was necessary to calibrate backscatter measurements of the four beams separately. Calibration was undertaken using the manufacturers suggested approach as described by Deines (1999). Comparison of backscatter measurements from the four beams showed that they agreed to within ±0.5 dB. The present result is substantially better than the between beam difference of 3.8 dB reported by Griffiths and Diaz (1996).

The presence of large differences in backscatter between ADCP beams raises the question of how data between beams should be averaged. If differences between beams is seen to occur and it is not caused by calibration errors then averaging the data together is inappropriate. The occurrence of directionality in backscatter can also complicate comparisons between ADCP data and that of conventional scientific echosounders as has been noted by Griffiths and Diaz (1996).

6 Acknowledgements

The following are thanked for their support of this work: the EU through RTD-contract no. MAS3-CT95-0031 (BASS), the Norwegian Research Council through grant no. 113809/122, and Bergen Large-Scale Facility for Marine Pelagic Food Chain Research.

Thanks are due to Kenneth G. Foote providing the opportunity to participate in herring survey cruises and to Lee R. Gordon who made available the RD Instruments WorkHorse Sentinel and FishMass 307 kHz systems for these experiments, and Dezhang Chu for the herring backscatter model results.

7 Appendix A: Beam Rotations

In a coordinate system aligned with the ADCP itself, the four beams of a downward looking RDI ADCP have unit vectors:

$$\begin{array}{lcccc} \vec{b1} & = & -sin(20) & 0 & -cos(20) \\ \vec{b2} & = & sin(20) & 0 & -cos(20) \\ \vec{b3} & = & 0 & sin(20) & -cos(20) \\ \vec{b4} & = & 0 & -sin(20) & -cos(20) \end{array} \quad (4)$$

defining their directions of orientation. In order to use the data in a "real world" coordinate system, these vectors must be corrected for the heading, pitch and roll of the instrument. The corrections matrices for heading pitch and roll are given as:

$$D = \begin{pmatrix} cos(h) & sin(h) & 0 \\ -sin(h) & cos(h) & 0 \\ 0 & 0 & 1 \end{pmatrix} \quad (5)$$

$$C = \begin{pmatrix} 1 & 0 & 0 \\ 0 & cos(p) & sin(p) \\ 0 & -sin(p) & cos(p) \end{pmatrix} \quad (6)$$

$$B = \begin{pmatrix} cos(r) & 0 & sin(r) \\ 0 & 1 & 0 \\ -sin(r) & 0 & cos(r) \end{pmatrix} \quad (7)$$

where, h is heading (counterclockwise from the [0 0 1] axis), r is roll, and p is pitch (in a right handed coordinate sense). The value of pitch reported by the ADCP must be corrected to the mathematical term using the relation;

$$p = tan^{-1}(tan(pt) \times cos(r)) \quad (8)$$

where pt is the pitch angle reported by the ADCP (RD Instruments (1998)).

The beam vectors (given by (4)) are corrected for heading pitch and roll as,

$$\vec{B1} = D \times B \times C \times \vec{b1}, \quad (9)$$

where $\vec{B1}$ is the world coordinate vector for beam 1. Corrections for the the other beam vectors are mathematically identical to Equation (9).

8 References

Ashjian, C.J., S.L. Smith, C.N. flagg, A.J. Mariano, W.J. Behrens, and P.V.Z. Lane, 1994: The influence of a Gulf Stream meander on teh distribution of zooplankton biomass in the Slope Water, the Gulf Stream, and the Sargasso Sea, described using a shipboard acoustic Doppler current profiler. Deep-Sea Research I, 41, 23-50.

Blaxter, J.H.S., and Batty, R.S., 1984: The herring swimbladder: loss and gain of gas. Journal of the Marine Biological Association of the United Kingdom, 64: 441-459.

Brierely, A.S., M.A. Brandon, J.L. Watkins 1998:, "An assessment of the utility of an acoustic Doppler current profiler for biomass estimation" *Deep-Sea Research I*, 45, 1555-1573.

Chu, D., J.M. Jech, and A. Lavery, 2003: Inference of shape and behavioral information of individual fish from echo trace analysis. Deep Sea Res. I, 50, 515-527.

Deines, K.L., 1999: Backscatter estimation using broadband acoustic Doppler current profilers. Proceedings of the IEEE Sixth Working Conference on Current Measurement, San diego.

Demer, D.A., M.Barange, A.J. Boyd, 2000. Measurements of three-dimensional fish school velocities with an acoustic Doppler current profiler. Fisheries Research, 47, 201-214.

Fielding, S., G. Griffiths, and H.S.J. Roe, 2004: The biological validation of ADCP acoustic backscatter through direct comparison with net samples and model predictions based on acoustic-scattering models. ICES Journal of Marine Science, in-press.

Flagg, C.N., and S.L. Smith, 1989: On the use of the acoustic Doppler current profiler to measure zooplankton abundance. Deep-Sea Research I, 36, 455-474.

Foote, K., and O. Nakken, 1978: Dorsal aspect target strength functions of six fishes at two ultrasonic frequencies. Fisken Hav. Ser. B 3: 1-96.

Gorska, N., and E. Ona, 2003: Modelling the acoustic effect of swimbladder compression in herring. ICES Journal of Marine Science, 60, 548-554.

Gordon, R.L., 1996: Acoustic Doppler Current Profilers: a practical primer, R.D. Instruments, San Diego, USA.

Griffiths, G., J.I. Diaz, 1996: Comparison of acoustic backscatter measurements from a ship-mounted Acoustic Doppler Current Profiler and an EK500 scientific echosounder. ICES Journal of Marine Science, 53. 487-491.

Griffiths, G., S. Fielding, H.S.J. Roe, 2002: "Biological-Physical-Acoustical interactions", *in* Biological-physical interactions in the sea, M.N. Hill, A.R. Robinson, J.J. McCarthy, B.J. Rothschild. 441-474.

Huse, I. and E. Ona, 1996: Tilt angle distribution and swimming speed of overwintering Norwegian spring spawning herring. ICES J. Mar. Sci., 53, 863-873.

Lee, K., T. Mukai, D. Kang, and K. Iida, 2004: Application of ADCP for krill density estimation. Journal of Fisheries Science, *accepted*.

RD Instruments, 1998: ADCP coordinate transformation. RD Instruments, San Diego, 27 pp.

Ressler, P.H., 2002: Acoustic backscatter measurements with a 153 kHz ADCP in the northeastern Gulf of Mexico: determination of dominant zooplankton and micronekton scatterers. Deep-Sea Research I, 49, 2035-2051.

Zedel, L., T. Knutsen, R. Patro, 2003: ADCP Observations of Herring Movement. ICES Journal of Marine Science, 60, 846-859.